Title page

# DEVELOPMENT OF SOLAR ISODOSE LINES: MERCATORIAN AND SPATIAL GUIDES FOR PRELIMINARY DESIGN AND INSTALLATION OF SOLAR FACILITIES

**Nnamchi, S. N***[1], Jagun, Z. O[2], Nnamchi, O. A[3], Onochie, U.[4], Mundu, M. M[5] and Ekanem, D. O.[6]

1. Department of Mechanical Engineering, SEAS, Kampala International University, P.O. Box 20000, Kampala, Uganda, stephen.nnamchi@kiu.ac.ug, ORCID; 0000-0002-6368-2913.
2. Department of Computer Engineering, OlabisiOnabanjo University, Ibogun, Nigeria, Jagun.zaid@oouagoiwoye.edu.ng, https://orcid.org/ 00000002-1544-0266
3. Department of Agricultural Engineering and Bio Resources, Michael Okpara University of Agriculture, Umudike, Umuahia, Nigeria, onyxhoni@yahoo.com, ORCID: https://orcid.org/0000-0003-4099-601X
4. Department of Mechanical Engineering, Alex Ekwueme Federal University Ndufu-Alike, P.M.B. 1010, Abakaliki, Nigeria, onochie.uche@funai.edu.ng, ORCID: https://orcid.org/0000-0002-2274-6394
5. Department of Physical Sciences, SEAS, Kampala International University, P.O. Box 20000, Kampala, Uganda, mundu.mustafa@kiu.ac.ug, ORCID; 0000-0003-1345-9999
6. Department of Mechanical Engineering, Alex Ekwueme Federal University Ndufu-Alike, P.M.B. 1010, Abakaliki, Nigeria, dianaekanem@yahoo.com, ORCID: https://orcid.org/**0000-0001-6986-8033**

**Abstract**

Mercatorian and spatial studies of solar power potential (SPP) provide technical guides for the preliminary design and installation of efficient photovoltaic plant. Modeling and simulation of the SPP were preceded by acquisition and processing of essential satellite and on-station data; clearness index, relative sunshine hours, latitude and longitude. The mercatorian SPP model was developed as a geometric function of latitude and longitude, whereas the spatial SPP model was developed with the application of the Haversine formula as a function of $x\ and\ y$ coordinates. The distributed and concentrated SPP contours were characterized by multiple isodose lines and a single maximum isodose line, respectively. The present geometric SPP model validated well with the measured SPP with insignificant error results ($1.26173E-06\ -\ 2.93324E$ - 05) for the study areas. The study shows the range of the concentrated SPP as; $743.7-757.5, 624.7-635.2, 543.8-557.5, 403.5-405.9\ W/m^2$ and the corresponding concentrated area is found as $29084.648, 15368.638, 1179.585\ and\ 635.7\ km^2$, for the Northern Region (NR), Eastern Region(ER), Central Region (CR) and Western Region (WR), respectively. Also, the districts within the concentrated areas of the $NR, ER, CRandWR$ in Uganda are listed in the table of results. The areas established are useful for preliminary design of solar facilities. Also, it is obvious that NR is a home for installation of efficient solar facilities based on the above results. Thus, the present work recommends for transmission of solar power to the study area not favored with high SPP and extension of the state-of-the-art to other locations yet to be studied.

**Keywords**

Isodoses, mercatorian, spatial, distributed and concentrated SPP, preliminary design, installation guide, solar facilities.

**Acknowledgement**

We do recognize the two main sources of data that were used in the study; NASA POWER and the Department of Physics, Makerere University, for providing the data used in the development and analysis of solar power potential models in Uganda.

∗1 Corresponding Author

# DEVELOPMENT OF SOLAR ISODOSE LINES: MERCATORIAN AND SPATIAL GUIDES FOR PRELIMINARY DESIGN AND INSTALLATION OF SOLAR FACILITIES

**Abstract**
Mercatorian and spatial studies of solar power potential (SPP) provide technical guides for the preliminary design and installation of efficient photovoltaic plant. Modeling and simulation of the SPP were preceded by acquisition and processing of essential satellite and on-station data; clearness index, relative sunshine hours, latitude and longitude. The mercatorian SPP model was developed as a geometric function of latitude and longitude, whereas the spatial SPP model was developed with the application of the Haversine formula as a function of $x\ and\ y$ coordinates. The distributed and concentrated SPP contours were characterized by multiple isodose lines and a single maximum isodose line, respectively. The present geometric SPP model validated well with the measured SPP with insignificant error results ($1.26173E-06\ -\ 2.93324E$ - 05) for the study areas. The study shows the range of the concentrated SPP as; $743.7-757.5, 624.7-635.2, 543.8-557.5, 403.5-405.9\ W/m^2$ and the corresponding concentrated area is found as $29084.648, 15368.638, 1179.585\ and\ 635.7\ km^2$, for the Northern Region (NR), Eastern Region(ER), Central Region (CR) and Western Region (WR), respectively. Also, the districts within the concentrated areas of the $NR, ER, CR\ and\ WR$ in Uganda are listed in the table of results. The areas established are useful for preliminary design of solar facilities. Also, it is obvious that NR is a home for installation of efficient solar facilities based on the above results. Thus, the present work recommends for transmission of solar power to the study area not favored with high SPP and extension of the state-of-the-art to other locations yet to be studied.

**Keywords**
Isodoses, mercatorian, spatial, distributed and concentrated SPP, preliminary design and installation guide, solar facilities.

## 1.0 Introduction

The industrial and domestic energy demand for the socioeconomic growth of the society is attracting exploitation of natural energy resources like the solar energy using helio-photovoltaic device in the conversion of solar to electrical energy. The potential of a place to hold a helio-photovoltaic device is predominantly defined by the magnitude of solar power potential or global solar radiation. The solar power potential is mathematically modeled to quantify its value where measurement is limited.

Generally, solar power potential (SPP) model is dominated by the direct linear relationship between the normalized SPP and the clearness index. Essentially, the clearness index signifies the intensity or magnitude of the cloud within the study area [1-3]. Besides, the popular model aforementioned, the artificial neural networks (ANN) models (linear and nonlinear) have been developed for the purposes of predicting solar power potential of different locations in the bid to satisfy the energy demand of the different locations [4-8]. Inclusively, the benefits of ANN include evaluation and monitoring of the solar resource potential and forecasting of solar energy potential [7, 9, 10], global predictions, location and design of solar energy systems [12-14]. Basically, the input parameters to SPP model include temperature, altitude and sunshine hours, longitude, clearness index, wind speed and extraterrestrial radiation [7, 9-17]. However, the ANN is dependent on the network availability which may not be available in all the locations, hence, the silent need to develop an encompassing and non-neural network model which this paper is expected to fill the gap.

Commonly, clearness index has been modeled as a linear function of relative sunshine hours [18-23]; quadratic function of relative sunshine hours [20, 24, 25] and multiple functions of relative sunshine hours and temperature, relative humidity, precipitation, latitude [17, 26-36]. Besides, the model development of

the SPP, the empirical studies of the SPP are achieved by stationing measurement equipment like pyranometer, pyrheliometer, sunshine recorders and geographic information systems, GIS [37-39], but the coverage is highly limited because of the high cost of extensive installation of recording equipment. However, the present work develops multiple variables and quadratic SPP model using relative sunshine hours, latitude and longitude. The relative sunshine hours designate the extraterrestrial condition of the study area, while the latitude and longitude designate the terrestrial characteristics of the study area (s). Uniquely, clearness index model encompasses both terrestrial and extraterrestrial conditions of the study areas against the bulk of clearness models in the literature [39], which are solely modeled on the extraterritorial characteristic of the study area (s).

Moreover, the present model distinctively formulates the relative sunshine hours as a geometric function of latitude and longitude, in the bid to make the SPP model to be mercatorian or sensitive to both latitude and longitude of the study areas (Lat., 1.3733° N; Long., 32.2903° E). Also, the present work transforms the mercatorian SPP model into the spatial model using the Haversine formula to generate SPP model dependent on the spatial coordinates $(x, y)$[40, 41]. Concertedly, the mercatorian and spatial models are employed in identifying concentrated SPP within the study area for the purpose of establishing or localizing mega solar power plant, which is one of the objectives of this paper. The present work is aimed at providing SPP distribution in the study areas for future and enhanced energy planning.

Obviously, the preliminary design and installation of solar facilities is highly technical. Thus, installing a solar facility based on the avalanche of the SPP or global solar radiation local or discrete data could result in the underperformance of the solar facility. The underperformance could be as a result of not installing the solar plant in the area highly concentrated with solar irradiance. This area is enclosed by a line of constant or equal solar irradiance, known as isodose line. The actual area with a highly concentrated isodose is determined from the contours of the SPP. This gives the actual or design area available for the installation of solar facility. Once the concentrated isodose and the area forming it are not employed in the preliminary design of the solar facilities, the plant is likely to underperform. Unfortunately, this information cannot be availed by the avalanche of satellite or station measured SPP data. This primary information could be obtained by developing the distributed and concentrated isodoses from the bulk of the satellite or measured data. The art of developing the distributed and concentrated SPP is presented in this paper. The isodose contours are presented in both mercatorian and spatial forms, the former is useful for identification of districts (places) which are favored with high SPP within the study areas. The latter is essential for determining the area and perimeter of the distributed and concentrated contours in the study areas. The area determined is useful for the preliminary design of solar facilities. Moreover, this paper presents the development of isodose lines or contours for determination of study area favored with concentrated SPP rather than the distributed SPP and to avail the concentrated isodose and the area enclosed by the concentrated isodose for the enhanced performance of solar facilities. Other sections of this work include; materials and methods basically the model formulation and analysis, results and presentation of the analysis, discussion of the results, conclusions and recommendations for further study.

### 1.1 Study Area

The study area covers the entire territory of Uganda, composed of four regions; the Northern Region (NR), the Eastern Region (ER), the Central Region (CR) and the Western Region (WR). Uganda is an equatorial sub-Saharan country, landlocked in the north by Southern Sudan, in the east by Kenya, in the west by Congo and in the south by Rwanda and Tanzania. By virtue of being an equatorial country, Uganda is suitable for installing solar facilities. According to Fig. 1, the NR region is composed of five sub-regions; West Nile, Acholi, Karamoja and Lango. The ER comprises of Teso, Elgon and East Central subregions. The CR is made up only Central sub-region. The Western and South Western form the WR.

## 2.0 Materials and Method

The materials and method are preceded with the acquisition of the essential and primary input data for the development of the SPP and normalized solar power potential (NSPP) models; the clearness index ($k_T$), relative sunshine hours ($rsh$), latitude ($\phi$), longitude ($\lambda$) from the National Aeronautic Space Administration (NASA) and Department of Physics, Makerere University furnished the satellite and on-station data, respectively. The satellite data were filtered and arranged in excel environment and later exported to OriginLab to obtain the coefficients of the SPP, NSPP, RSH, $and\ k_T$ models. The methodology is algorithmized in Figs. 2 and 3. Sequentially, the SPP model is developed as a function of $k_T$, the $k_T$ model is developed as a function of the RSH, $\phi$ and $\lambda$. In the same vein, the RSH model is established as a function of $\phi$ and $\lambda$. Subsequently, the RSH model is nested into the $k_T$ model, while the $k_T$ model is nested into the SPP model to obtain the mercatorian SPP model (MSPP). Furthermore, the mercatorian coordinates are converted into the Cartesian (spatial) coordinates ($x, y$) to obtain the equivalent spatial SPP model (SSPP) using Haversine formula. Thus, the MSPP and SSPP models are formulated to fulfil the set objective of the present study; a mercatorian and spatial study. The output parameters of the analysis (flow chart) are; $SPP$, $areas$ ($A_d$ and $A_c$), $\phi$, $\lambda$, $x$ and $y$. These essential results are used in the detailed investigation of the solar power distribution (Fig. 2) and concentration (Fig. 3) within the study areas.

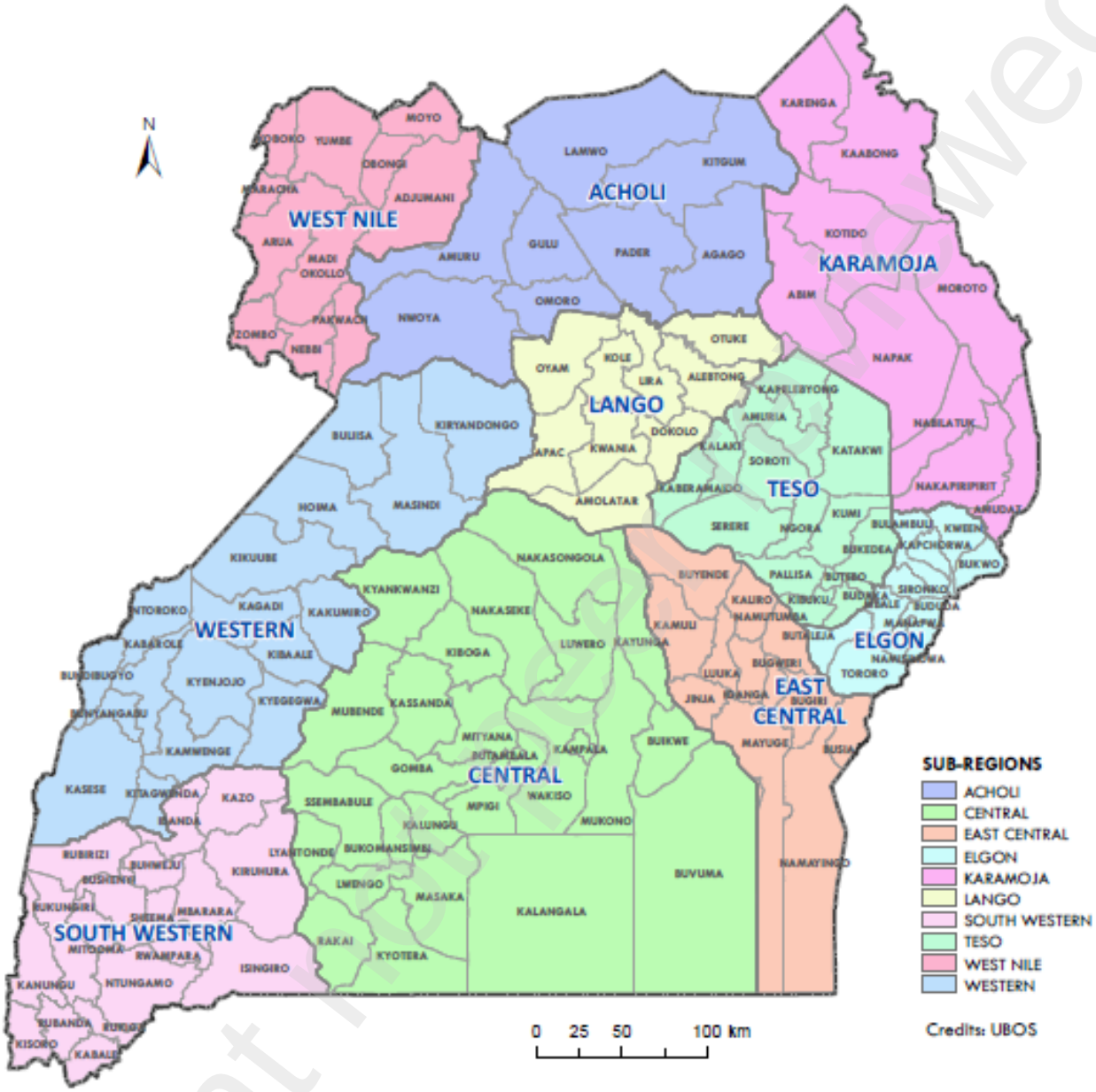


NR ≡ {West Nile, Acholi, Karamoja, Lango}; ER ≡ {Teso, Elgon, East Central}; CR ≡ {Central}; WR ≡{Western, South Western}

**Fig. 1**. Map of the study areas (NR, ER, CR, WR)

**Source**: https://reliefweb.int/sites/reliefweb.int/files/resources/76380.pdf

### 2.1 Description of flowcharts

The development of the isodose lines is accomplished by the distributed and concentrated SPP flowcharts in Fig. 2 and Fig. 3, respectively.

### 2.1.1 The distributed SPP flowchart

The flowchart in Fig. 2 is initiated by inputting the latitude ($\phi_i$), longitude ($\lambda_i$), relative sunshine hours ( $RSH_i$), measured/satellite; clearness index ($K_{T,i}$) and solar power potential ($SPP_i$) for the four regions {NR, ER, CR, WR}. The maximum and minimum of $\phi_i$ and $\lambda_i$ are sorted ($\phi_{min}$, $\lambda_{min}$, $\phi_{max}$ , $\lambda_{max}$). These extreme coordinated are used to establish the distributed boundary conditions. Then, clearness index ($K_T$) and modified clearness index ($K_T^{'}$) models are developed using the input data. The dimensionless SPP is directly proportional to modify clearness index ($K_T^{'}$). The mercatorian coordinates are converted into spatial coordinates by the aid of Haversine formula. Essentially, the mercatorian SPP corresponds to the spatial SPP. Also, the emergence of spatial coordinates helps in the computation of distributed and concentrated areas. Lastly, the simulated SPP is validated against the measured SPP. Once, the iteration is executed for the four regions of the study areas. Then, the important output results in the regions are displayed and the algorithm stopped.

### 2.1.2 The concentrated SPP flowchart

The concentrated SPP flowchart (Fig. 3) is a subset of the distributed SPP flowchart (Fig. 2) representing areas with maximum concentrated SPP. The concentrated SPP flowchart is a simple algorithm solely responsible for identifying districts with maximum concentrated SPP. The algorithm starts by accepting initial input data as in the distributed SPP flowchart. The algorithm uses four boundaries equalities (forming the boundaries of the maximum concentrated SPP or isodose line enclosed boundaries) in identifying the favourable districts. At the same time, it rejects the districts outside the maximum concentrated SPP. On completion of the iterations, the districts with maximum concentrated SPP and their mercatorian coordinates are outputted in Fig. 3.

### 2.2 Formulation of solar power potential (SPP) model

The SPP-model is formulated on direct mathematical proportionality between the solar power potential and clearness index in Eq. (1). The solar power potential (SPP) is synonymous to global solar radiation (H) reaching the horizontal or an inclined surface. It is a ratio of the terrestrial to extraterrestrial solar power reaching a horizontal surface, which is equivalent to the clearness index of a location [36, 42] in Eq. (1)

$$\frac{SPP}{SPP_0} = \frac{\overline{SPP}}{\overline{SPP_0}} = \frac{H}{H_0} = \frac{\overline{H}}{\overline{H_0}} = k_T \tag{1}$$

where, $H$ is the monthly daily solar irradiance reaching a horizontal surface, $H_0$ is the corresponding monthly average daily extraterrestrial solar irradiance on the same location, whereas $\overline{H}$ is the average monthly average daily solar irradiance reaching a horizontal surface and $\overline{H}_0$ is the corresponding average monthly average daily extraterrestrial solar irradiance in the same location, $k_T$, is the clearness index of a given location.

The clearness index, $k_T$ is modelled as a function of latitude and relative sunshine hours ($RSH$) in accordance with [43] as represented in Eq. (2). The previous clearness index models for the study area were developed by Mubiru et al [10], Rijix and Huskley[11]. Mubiru et al [10] recommend quadratic model as the best of their models for the study area in Eq. (2)

$$k_T = a_0 + a_1 RSH + a_2 RSH^2 \quad (-) \tag{2}$$

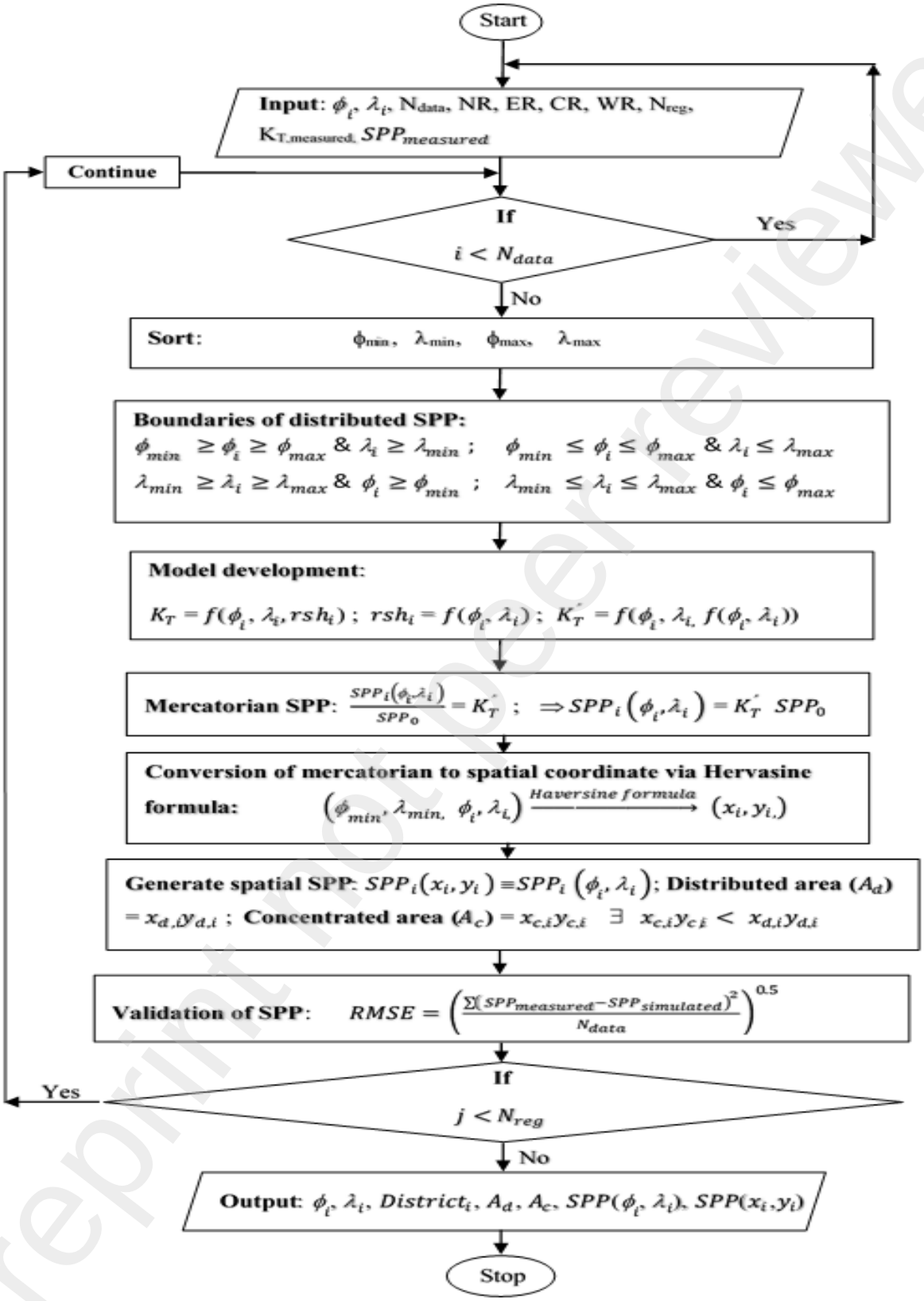


**Fig. 2.** Distributed SPP flowchart

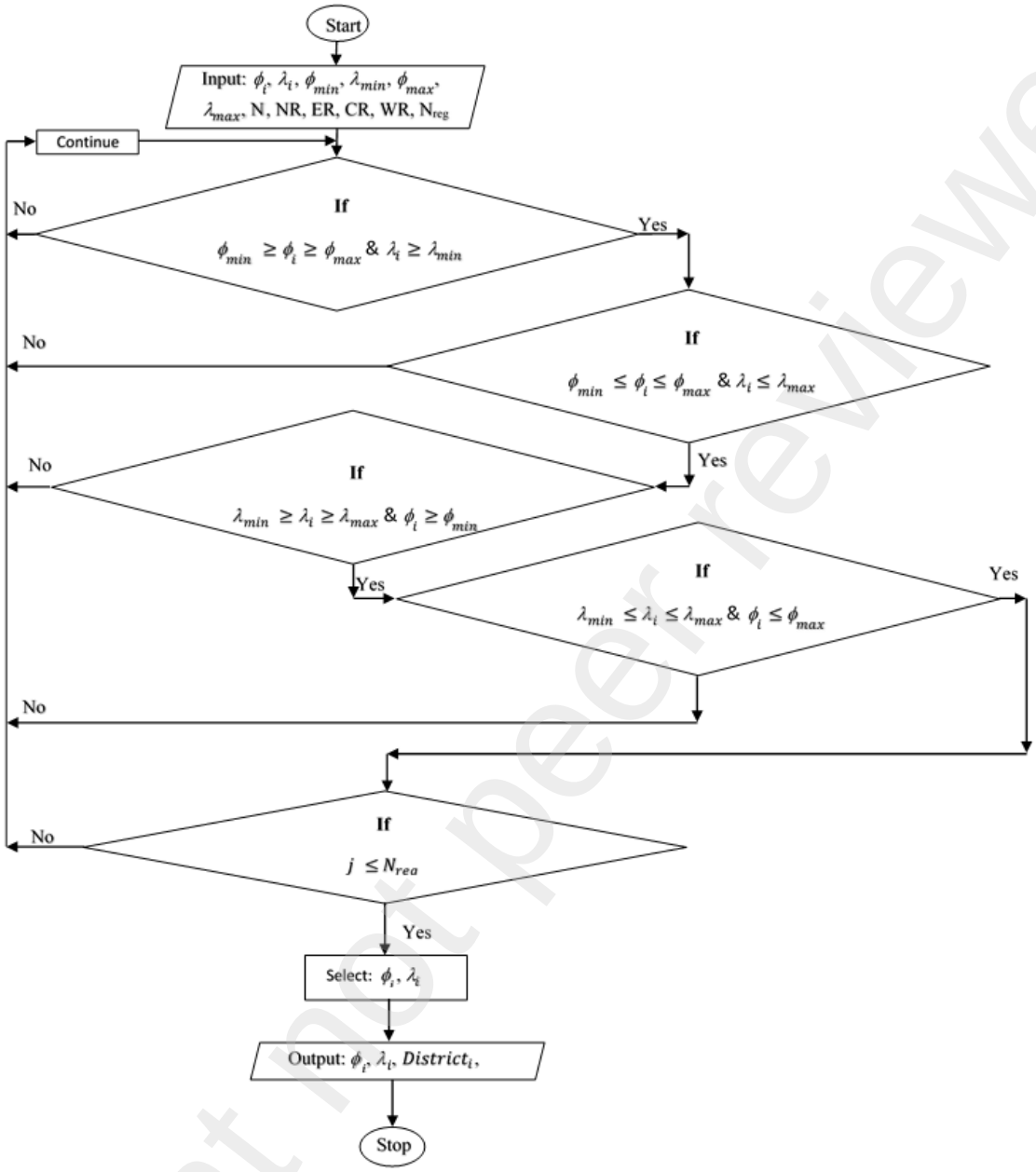


**Fig. 3.** Concentrated SPP flowchart

where $a_{i,}$ $i = 0, 1, 2$ are coefficients of Eq. (2) and $rsh$ is the relative sunshine hours.
Rijix and Huskley [11] recommend a linear model for the study area in Eq. (3)

$$k_T = b_0 + b_1 RSH \quad (-) \tag{3}$$

where $b_i$,$i = 0, 1$ are coefficients of Eq. (3)

However, the present work has proposed more robust clearness index model, which incorporates the latitude, longitude and relative sunshine hours of the study areas in Eq. (4) as;

$$k_T = c_0 + c_1\cos\phi + c_2 sin\lambda + c_3 RSH + c_4 cos\phi.sin\lambda + c_5 RSH cos\phi + c_6 RSH.sin\lambda + c_7\lambda + c_9 RSH^2 \quad (-) \tag{4}$$

where, $c_i$, $i = 0, 1, 2, ..., 9$ are coefficients of cubic $k_T$ model, $\phi$ is the latitude and $\lambda$ is the longitude within the study area.

The $RSH$ indicator is defined with latitude and longitude quadratic function in Eq. (5) as

$$rsh = d_0 + d_1\cos\phi + d_2 sin\lambda + d_3\cos\phi.sin\lambda + d_4\cos^2\phi + d_5\sin^2\lambda \tag{5}$$

where, $d_i$, $i = 0, 1, 2$ are coefficients of the quadratic $RSH$ model, $\lambda$ is the longitude of a given location. Substituting Eq. (5) into Eq. (4) gives Eq. (6) which depends on the latitude and longitude of the location

$$k_T = c_0 + c_1\cos\phi + c_2 sin\lambda + c_3\left(d_0 + d_1\cos\phi + d_2 sin\lambda + d_3\cos\phi.sin\lambda + d_4\cos^2\phi + \right. \\ cos\phi.sin\lambda + c_5\left(d_0 + d_1\cos\phi + d_2 sin\lambda + d_3\cos\phi.sin\lambda + d_4\cos^2\phi + d_5\sin^2\lambda\right).cosq \\ \left(d_0 + d_1\cos\phi + d_2 sin\lambda + d_3\cos\phi.sin\lambda + d_4\cos^2\phi + d_5\sin^2\lambda\right).sin\lambda + c_7\cos^2\phi + c \\ \lambda + c_9\left(d_0 + d_1\cos\phi + d_2 sin\lambda + d_3\cos\phi.sin\lambda + d_4\cos^2\phi + d_5\sin^2\lambda\right)^2 \quad (-) \tag{6}$$

Equation (1) is modified with Eq. (6) in Eq. (7a), which is a mercatorian representation of the SPP-model depending on the latitude and longitude of a location.

$$\frac{SPP}{\overline{SPP_0}} = \frac{\overline{SPP}}{\overline{SPP_0}} \equiv \frac{H}{H_0} = \frac{\overline{H}}{\overline{H_0}} = c_0 + c_1\cos\phi + c_2 sin\lambda + c_3 \\ \left(d_0 + d_1\cos\phi + d_2 sin\lambda + d_3\cos\phi.sin\lambda + d_4\cos^2\phi + d_5\sin^2\lambda\right) + c_4 cos\phi.sin\lambda + c \\ + d_1\cos\phi + d_2 sin\lambda + d_3\cos\phi.sin\lambda + d_4\cos^2\phi + d_5\sin^2\lambda).cos\phi + c_6(d_0 + d_1\cos \\ + d_2 sin\lambda + d_3\cos\phi.sin\lambda + d_4\cos^2\phi + d_5\sin^2\lambda).sin\lambda + c_7\cos^2\phi + c_8 sin^2\lambda + c_9( \\ + d_1\cos\phi + d_2 sin\lambda + d_3\cos\phi.sin\lambda + d_4\cos^2\phi + d_5\sin^2\lambda)^2 \quad (-) \tag{7a}$$

Similarly, Muburi et al [10] proposed SPP model in Eq. (7b) as

$$\frac{SPP}{SPP_0} = \frac{\overline{SPP}}{\overline{SPP_0}} \equiv \frac{H}{H_0} = \frac{\overline{H}}{\overline{H_0}} = a_0 + a_1 RSH + a_2 RSH^2 = 0.288 + 0.154 RSH + 0.448 RSH^2 \quad (-) \tag{7b}$$

Equivalent SPP model by Rijix and Huskley [11] is provided in Eq. (7c) as

$$\frac{SPP}{SPP_0} = \frac{\overline{SPP}}{\overline{SPP_0}} \equiv \frac{H}{H_0} = \frac{\overline{H}}{\overline{H_0}} = b_0 + b_1 RSH \quad = 0.24 + 0.47 RSH \quad (-) \tag{7c}$$

The average daily, monthly extraterrestrial solar irradiance is given in Eq. (8) [44] as follows;

$$H_0 = I_{sc}\left[1 + 0.033\cos\left(\frac{360n}{365}\right)\right]\left[\cos\phi\cos\delta\sin\omega_s + \frac{2\pi\omega_s}{360}\sin\phi\sin\delta\right] \\ \exists\ SPP_0 \equiv H_0 \tag{8}$$

where $I_{sc}$ is the solar constant $(1367\ Wm^{-2})$, $n$ is the number of days starting from first January, $\omega_s$ is the sunset hour angle, $\phi$ is the latitude of a given location and $\delta$ is the angle of declination defined in Eq. (9) according to [44] as

$$\delta = 23.45\sin\left[360\left(\frac{284+n}{365}\right)\right] \tag{9}$$

and $\omega_s$ is sunset hour angle, which is expressed in Eq. (10) as

$$\omega_s = cos^{-1}(-\tan\delta\tan\phi) \tag{10}$$

The mercatorian model in Eq. (6) is converted into spatial form with the Haversine formula to determine the geographical distance, $d_{i,j}$ between any two locations [45-49] at regional levels as in Eq. (11)

$$d_{ij} = 2R_{Earth}.Atan2\left[\left(\sin^2\left(\frac{\phi_2-\phi_1}{2}\right)+\cos\phi_1\cos\phi_2\sin^2\left(\frac{\lambda_2-\lambda_1}{2}\right)\right)^{0.5},\left(1-\left(\sin^2\left(\frac{\phi_2-\phi_1}{2}\right)+\cos\phi_1\cos\phi_2\sin^2\left(\frac{\lambda_2-\lambda_1}{2}\right)\right)\right)^{0.5}\right] \tag{11}$$

$$\exists x_{i,1} = x_{i-1,1} + d_{i,1};\ y_{1,j} = y_{1,j-1} + d_{1,j}$$

where $R_{Earth}$ is the radius of the Earth (a perfect sphere) equal to 6371 $km$ [45, 50-52], $L_{ij}(km)$ is the distance separating the two locations; $(\phi_1, \lambda_1)\ and\ (\phi_2, \lambda_2)$ are the latitudes and longitudes of the locations, respectively, $x$ (km) is distance in x-direction and $y$ (km) is distance in y-direction.

Equation (7) is validated with the measured SPP using root mean square error, RMSE in Eq. (12)

$$RMSE = \left(\frac{(SPP_{measured} - SPP_{simulated})^2}{n}\right)^{0.5} \tag{12}$$

where SPP is the solar power potential $(W/m^2)$ and $n\ (-)$ is the number of data observed.

The percentage of concentration of the SPP (PC_SPP) in the regions is defined in Eq. (13) as

$$\text{PC\_SPP} = \frac{SPP\ concentrated\ area}{SPP\ distributed\ area} \times 100 \quad (\%) \tag{13}$$

**3.0 Results and Discussions**

The results are sequentially presented both in tables and figures and duly discussed as follows:

The normalized solar power potential ($NSPP$) models in Eqs. (6 and 7) are represented by second order geometric equation with the coefficients ($c_i, i = 1, ..., 9$ in Table 1) for the regions (northern, eastern, central and western). The nested coefficients ($d_i, i = 1, ..., 5$ in Table 2) designate the $RSH$ in Eqs. (4 and 5). The coefficient of determination for the models is approximately one. This indicates a strong association between the $NSPP$ and mercatorian indicators (latitude and longitude). Further, the results substantiate the fact that mercatorian variables are properly selected and truly reflects the SPP and NSPP [15, 24]. The $NSPP\ or\ SPP$ model is equivalent to the clearness index in Eqs. (1 and 7) which is a nonlinear geometric function of the relative sunshine hours, latitude and longitude of the study area as shown in Tables1 and 2 with a strong coefficient of determination buttressing the fact that the latitude and longitude explicitly represent the relative sunshine hours.

Substituting the relative sunshine hours (Eq. (5)) into Eq. (4) makes Eq. (6) to be dependent on the latitude and longitude. Thus, the $NSPP\ or\ SPP$ could be computed for a specified latitude and longitude. Therefore,

the $NSPP\ or\ SPP$ was developed and computed on a regional basis. The areas with a high $NSPP\ or\ SPP$ are obviously depicted in the mercatorian plot [15, 24]. Regionally, Figs. 3 – 6 present both the distributed and concentrated SPP for $NR, ER, CR\ and\ WR$, respectively. According to Fig. 4, $NR$ is concentrated with SPP ($743.7 \leq SPP \leq 757.5\ Wm^{-2}$). Considering the selected districts within the $NR$ (Abim Agago, Alebtong, Amolatar, Amudat, Amuru, Apac, Dokolo, Gulu, Kaabong, Kole, Lira, Moroto, Nakapiripirit, Napak, Nebbi, Nwoya, Omoro, Otuke, Oyam, Pader, Pakwach and Zombo in Table 4), indicates that nonlinear SPP model (Eq. (7)) is effective for determining quality SPP data for the development of isodose lines in the region [14]. Broadly, Fig. 4 portrays that the SPP model for the Eastern Region, which is capable of identifying the following concentrated districts; Bududa, Bukwo, Kapchorwa, Kween, Manafwa, Mbale, Ngora, Serere, Soroti, Kaberamaido and Katakwi in Table 3. Evidently, these districts are endowed with SPP ($624.7 \leq SPP \leq 635.2\ Wm^{-2}$) and should be targeted for installation of solar facilities. However, the present solar power plant in Tororo district is outside the favored districts within the Eastern Region. Thus, Tororo plant cannot generate much power relative to the identified districts in the region. For all intents and purposes, the solar power developers and planners should concentrate on the identified districts in order to boost power generation in the nation (Uganda).
Correspondingly, Fig. 5 has identified the following districts; Kyankwanzi, Nakaseke, Kiboga, Kayunga and Nakasongola with SPP ($543.8 \leq SPP \leq 557.5\ Wm^{-2}$) and should be included in the solar exploitation list. Consistently, Fig. 6 identified Kisoro district with concentrated SPP ($403.5 \leq SPP \leq 405.9\ Wm^{-2}$), however, it should not be listed in the solar exploitation list due to the low value of the SPP reported.

Moreover, Table 3 and Eq. (13) provide the concentrated (and distributed) SPP areas, which are useful for the preliminary design of solar facilities as follows: 29084.648(100800), 15368.638(37050), 1179.585(26790) and 635.7(84760) $km^2$ for NR, ER, CR and WR, respectively. Offset designs will eventually culminate in underperformance of solar plants. These results show that NR is exceptionally endowed with highest SPP and a maximum expanse of land for installing solar facilities, followed by ER, then, CR. Installation of solar facility should be discouraged in the WR as the magnitude and the expanse of concentrated SPP is the least recorded among other regions. Furthermore, Figs. 8-11 present the validation of the present and past SPP models in the study areas (NR, ER, CR and WR). The present model is in good agreement with the measured data than the previous models. This fact could be supported by Root Mean Square Error (RMSE) result (in Table 5). The RMSE of the present work compared to those of Rijix and Huskley [11] and Mubiru et al [10] is quite insignificant which implies that the present model is more robust for prediction of the SPP, development of concentrated and distributed SPP isodose lines for the study areas. Notably, Figs. 8, 10-11 supported the linear relationship between $SPP$ and $K_T$ for NR, CR and WR, respectively. According to Muburi et al [10] indicates that the atmosphere in these regions is unpolluted, Conversely, Fig. 9 does not portray a linear relationship between $SPP$ and $K_T$ in the ER. By implication the atmosphere in the region is polluted. Considering the phenomenon in NR, CR and WR (Figs. 8, 10 and 11, respectively), the source of pollution is definitely external, which is likely to be attributed to industrial activities in the neighboring country, Kenya.

Based on the SPP result obtained in this study, the present work has shown that the installation of solar power plant in the Central and Western Regions will not favor optimal power generation, thus, it is recommended to install bulk of solar facilities in the Northern and Eastern Regions which have high SPP values and SPP concentrated areas [28].Pertinently, Figs.4b-7b present the conversion of the mercatorian SPP model into the corresponding spatial SPP model with the aid of a Haversine formula [45-49]. Precisely, these figures give the actual dimensions of the districts with highest SPP. This information is useful in mapping out the boundaries of the identified districts for the accurate installation of prospective solar power plants.

**Table 1. Coefficients of Eq. (7),normalized solar power potential**

| Coefficient | Regions | | | |
|---|---|---|---|---|
| | $NR$ | $ER$ | $CR$ | $WR$ |
| $c_0$ | 4.84E-10 | -3.368E-09 | -5.07E-08 | 1.073E-08 |
| $c_1$ | 2.71E-01 | 2.707E-01 | 3.25E-01 | 2.707E-01 |
| $c_2$ | 3.23E-11 | -2.989E-11 | -4.00E-10 | 1.218E-10 |
| $c_3$ | 5.20E-01 | 5.200E-01 | 6.24E-01 | 5.200E-01 |
| $c_4$ | -3.28E-11 | 2.933E-11 | 4.00E-10 | -1.227E-10 |
| $c_5$ | 2.52E-11 | -4.768E-11 | -2.33E-10 | 1.701E-10 |
| $c_6$ | -9.28E-13 | -4.053E-14 | 1.64E-12 | -2.051E-12 |
| $c_7$ | 4.89E-10 | -3.357E-09 | -5.08E-08 | 1.072E-08 |
| $c_8$ | 9.15E-13 | 5.403E-13 | -1.15E-12 | 1.846E-12 |
| $c_9$ | 2.25E-13 | -1.609E-13 | -4.05E-13 | 9.211E-13 |
| $R^2$ | 1.0000 | 1.0000 | 1.0000 | 1.0000 |

**Table 2. Coefficients of Equation (5), relative sunshine hours**

| Coefficient | Regions | | | |
|---|---|---|---|---|
| | $NR$ | $ER$ | $CR$ | $WR$ |
| $d_0$ | -35618.944 | 44.1060 | 159668.0946 | 131.06030 |
| $d_1$ | 72085.362 | -87.6274 | -322779.5894 | -261.68895 |
| $d_2$ | -1395.893 | -0.0036 | 6908.6060 | -0.03274 |
| $d_3$ | 1455.681 | 1.0001 | -6996.5588 | 1.00021 |
| $d_4$ | -36483.021 | 43.5224 | 163134.3608 | 130.63689 |
| $d_5$ | -51.959 | 0.0031 | 86.1706 | 0.03212 |
| $R^2$ | 0.8000 | 1.0000 | 0.8000 | 1.0000 |

**Table 3. Distribution and concentration of solar power potential in Figs. 4 - 7**

| Region | Distributed area ($km^2$) | Concentrated area ($km^2$) | Percentage of concentration (%) | Remarks |
|---|---|---|---|---|
| $NR$ | 100,800 | 29084.648 | 28.85 | Based on Fig. 4 |
| $ER$ | 37,050 | 15368.638 | 41.48 | Based on Fig. 5 |
| $CR$ | 26,790 | 1179.585 | 4.37 | Based on Fig. 6 |
| $WR$ | 84,760 | 635.7 | 0.75 | Based on Fig. 7 |

**Table 4. Districts concentrated with solar power potential in Figs. 4 - 7**

| Region | $\phi min$ | $\phi max$ | $\lambda min$ | $\lambda max$ | Districts captured by concentrated isodose line | Conc. SPP ($W/m^2$) | Remarks |
|---|---|---|---|---|---|---|---|
| $NR$ | 1.63 | 2.96 | 19.3 | 35.0 | Abim Agago, Alebtong, Amolatar, Amudat, Amuru, Apac, Dokolo, Gulu, Kaabong, Kole, Lira, Moroto, Nakapiripirit, Napak, Nebbi, Nwoya, Omoro, Otuke, Oyam, Pader, Pakwach, Zombo | 743.7-757.5 | Based on Fig. 3 |
| $ER$ | 0.28 | 2.00 | 34.5 | 34.7 | Bududa, Bukwo, Kapchorwa, Kween, Manafwa, Mbale, Ngora, Serere, Soroti, Kaberamaido, Katakwi | 624.7-635.2 | Based on Fig. 4 |
| $CR$ | 0.91 | 1.30 | 32.7 | 33.3 | Kyankwanzi, Nakaseke, Kiboga, Kayunga, Nakasongola | 543.8-557.5 | Based on Fig. 5 |
| $WR$ | -0.75 | -0.32 | 31.9 | 32.0 | Kisoro | 403.5-405.9 | Based on Fig. 6 |

**Table 5. Validation of solar power potential in the study areas Figs. 8 - 11**

| Region | Root mean square error (RMSE) | | | Remarks |
|---|---|---|---|---|
| | Previous SPP models | | Present SPP model | |
| | Rijix and Huskley (1964) | Mubiru et al (2007) | Present work | |
| ***NR*** | 75.81527 | 56.52517 | 1.26173E-06 | Based on Fig. 8 |
| ***ER*** | 60.20549 | 41.43285 | 6.73559E-06 | Based on Fig. 9 |
| ***CR*** | 45.8118 | 45.6332 | 2.93324E-05 | Based on Fig. 10 |
| ***WR*** | 36.31769 | 38.88739 | 1.47631E-05 | Based on Fig. 11 |

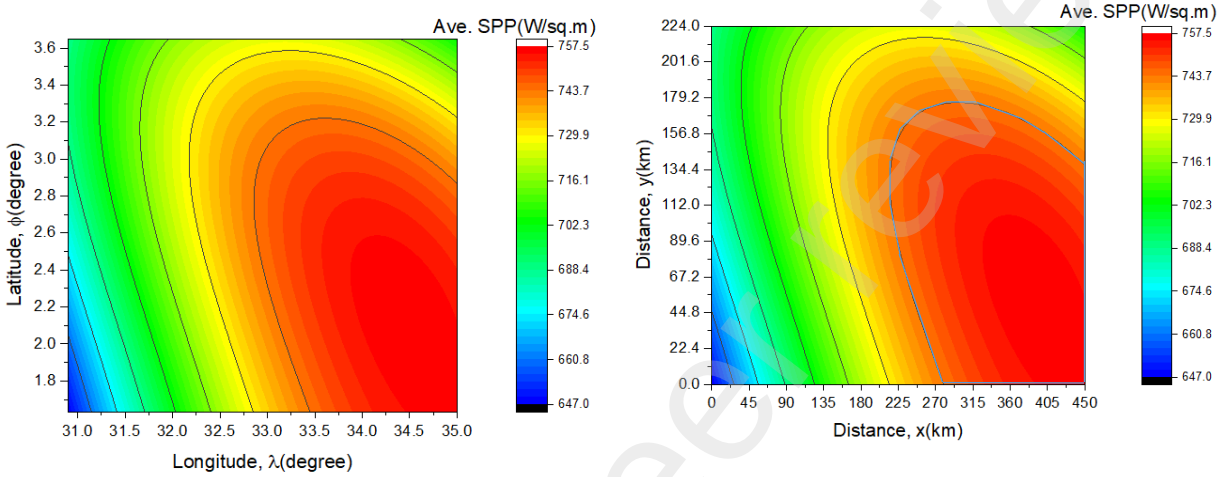


(a) Mercatorian isodoses (b) Spatial isodoses

**Fig. 4. Mercatorian and spatial distribution of solar power potential for Northern Region**

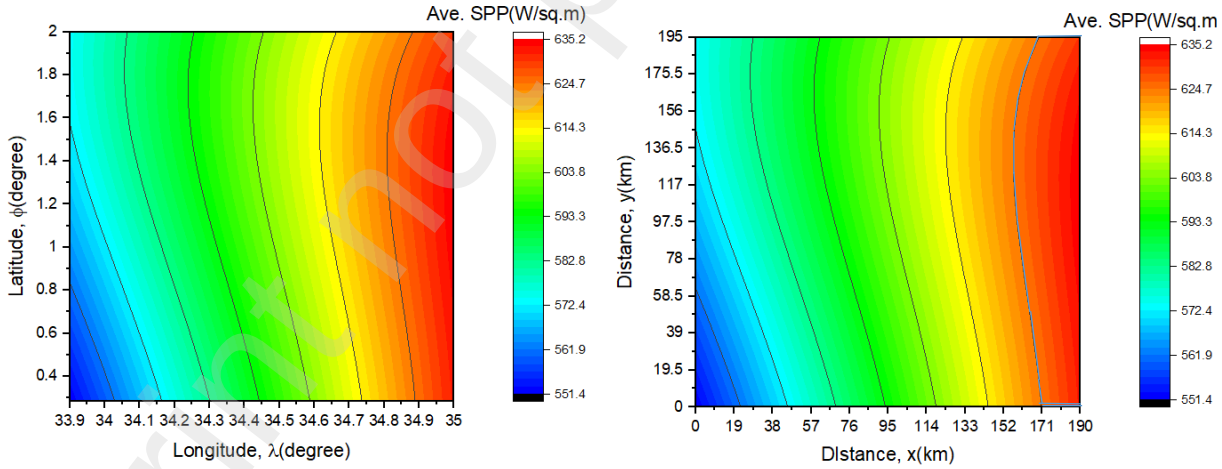


(a) Mercatorian isodoses (b) Spatial isodoses

**Fig. 5. Mercatorian and spatial distribution of solar power potential for Eastern Region**

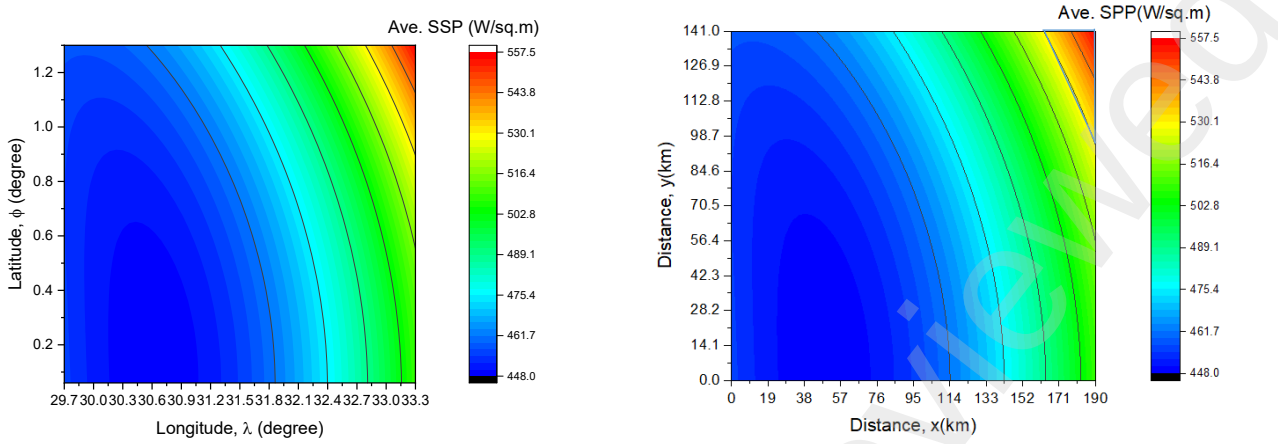


(a) Mercatorian isodoses (b) Spatial isodoses

**Fig. 6. Mercatorian and spatial distribution of solar power potential for Central Region**

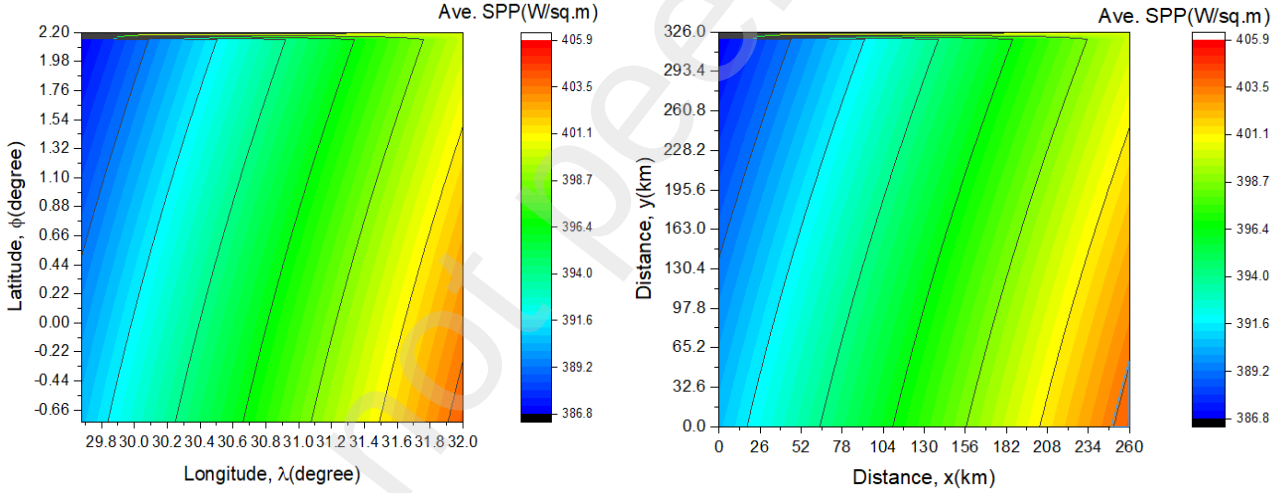


(a) Mercatorian isodoses (b) Spatial isodoses

**Fig. 7. Mercatorian and spatial distribution of solar power potential for Western Region**

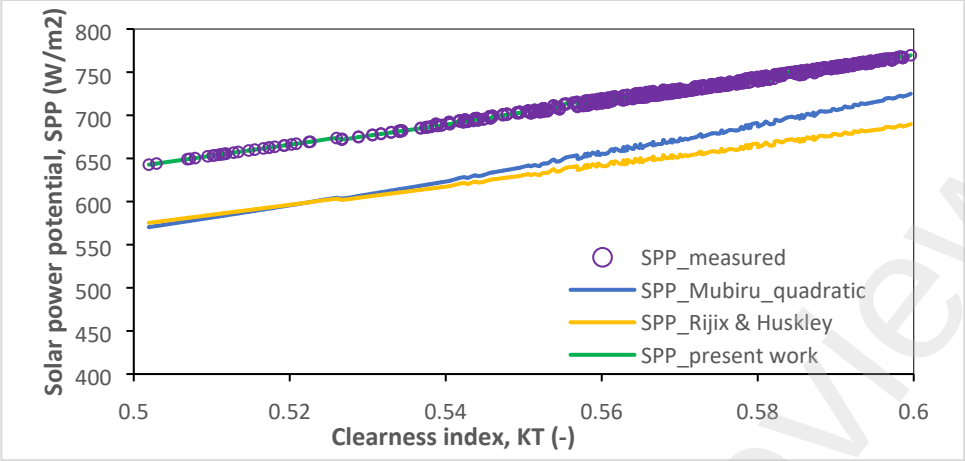


**Fig. 8. Reliability of solar power potential on clearness index for Northern Region**

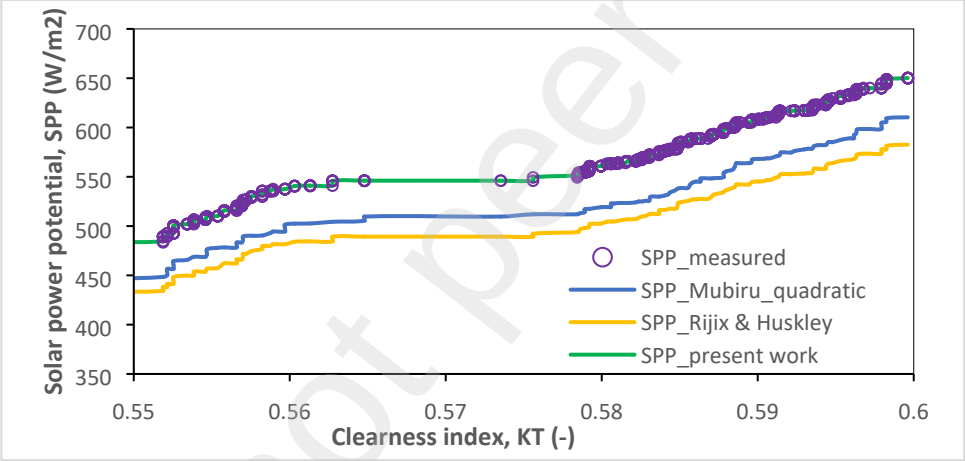


**Fig. 9. Response of solar power potential to clearness index for Eastern region**

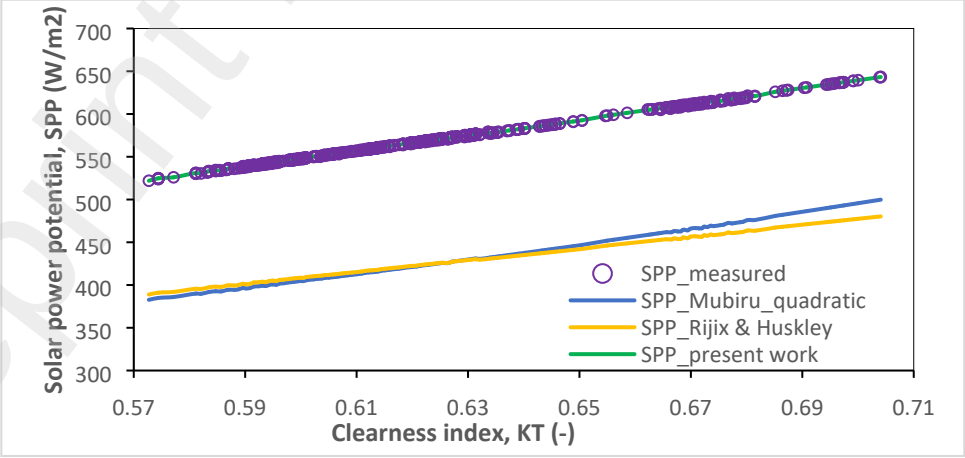


**Fig. 10. Reliance of solar power potential on clearness index for Central Region**

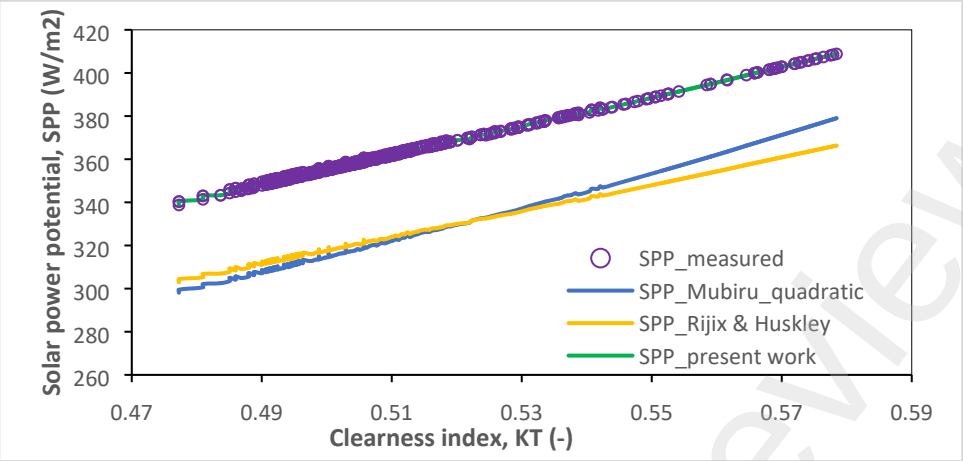


**Fig. 11. Dependence of solar power potential on clearness index for Western Region**

**4.0 Conclusion**

The present study has developed isodose lines in mercatorian and spatial coordinates as guides for preliminary design and installation of solar facilities. The distributed SPP contour is made of multiple isodose lines showing the magnitude or variation of the SPP in the study areas, whereas the concentrated SPP is characterized with the single highest isodose lines formed in the distributed SPP contour. The concentrated area is the main target for setting up high performing solar facilities. The results show the range of concentrated SPP as; 743.7-757.5, 624.7-635.2, 543.8-557.5, 403.5-405.9 W/m$^2$ for NR, ER, CR and WR, respectively. The concentrated area is found as 29084.648, 15368.638, 1179.585 and 635.7 km$^2$, for NR, ER, CR and WR, respectively. These results show that Northern Region, NR, is the most suitable home for the installation of solar facilities due to high magnitude of the SPP and wider concentrated area of the SPP. The NR is followed by ER and CR in terms of magnitude of the SPP and concentrated area of the SPP. Obviously, WR region is associated with the lowest SPP and concentrated area of the SPP, thus, solar facilities cannot be installed in the WR. The districts found in the concentrated area of NR are; Abim Agago, Alebtong, Amolatar, Amudat, Amuru, Apac, Dokolo, Gulu, Kaabong, Kole, Lira, Moroto, Nakapiripirit, Napak, Nebbi, Nwoya, Omoro, Otuke, Oyam, Pader, Pakwach and Zombo. Those found in the concentrated area of ER are; Bududa, Bukwo, Kapchorwa, Kween, Manafwa, Mbale, Ngora, Serere, Soroti, Kaberamaido and Katakwi. The districts identified in the concentrated area of the CR are; Kyankwanzi, Nakaseke, Kiboga, Kayunga and Nakasongola. However, the WR has Kisoro district as the only district with highest SPP in the WR.

Moreover, the present SPP models in mercatorian and spatial coordinates are quite robust as they recorded negligible value of RMSE relative to previous models by Muburi et al [10] and Rijix and Huskley [11]. Thus, the present model demonstrated strong agreement with the measured SPP data compared to the previous models. Hence, the isodose lines developed through this model is reliable for the guided installation of solar facilities in the study area. The linear relationship demonstrated by SPP and the clearness index in NR, CR and WR support the fact that the atmosphere in these regions is not polluted. However, the ER portrayed a nonlinear relationship between the SPP and clearness index, indicating that the atmosphere is polluted. In as much as the surrounding regions (NR and CR) are not polluted. Thus, this paper suggests that ER region is being polluted by the industrial activities of neighboring country (Kenya).

Furthermore, this study should be adopted by energy planners for improvement of power supply in the study areas (NR, ER and CR). The power generated from these areas should be transmitted to WR in order to meet its power requirements. Besides, this study could be replicated in other study areas in order to enhance power generation in a prospective study area.

**References**


1. Adeniji, N., J. Akinpelu, S. Adeola, and J. Adeniji, *Estimation of global solar radiation, sunshine hour distribution and clearness index in Enugu, Nigeria.* Journal of Applied Sciences Environmental Management, 2019. **23**(2): p. 345-349.
2. Kabir, E., P. Kumar, S. Kumar, A.A. Adelodun, and K.-H. Kim, *Solar energy: Potential and future prospects.* Renewable Sustainable Energy Reviews, 2018. **82**: p. 894-900.
3. Muneer, T., S. Etxebarria, and E. Gago, *Monthly averaged-hourly solar diffuse radiation model for the UK.* Building Services Engineering Research Technology, 2014. **35**(6): p. 573-584.
4. Chapman, C.A., K. Valenta, T.R. Bonnell, K.A. Brown, and L.J. Chapman, *Solar radiation and ENSO predict fruiting phenology patterns in a 15-year record from Kibale National Park, Uganda.* Biotropica, 2018. **50**(3): p. 384-395.
5. Avellino, O.W.K., F. Mwarania, A.-H.A. Wahab, K.T. Aime, and r. publications, *Uganda solar energy utilization: Current status and future trends.* Published in international journal of scientific, 2018. **8**(3).
6. Twaha, S., M.A. Ramli, P.M. Murphy, M.U. Mukhtiar, and H.K. Nsamba, *Renewable based distributed generation in Uganda: Resource potential and status of exploitation.* Renewable Sustainable Energy Reviews, 2016. **57**: p. 786-798.
7. Yesilbudak, M., M. Çolak, and R. Bayindir. *A review of data mining and solar power prediction*. in *2016 IEEE International Conference on Renewable Energy Research and Applications (ICRERA)*. 2016. IEEE.
8. Khogali, A., O. Albar, and B. Yousif, *Wind and solar energy potential in Makkah (Saudi Arabia)—comparison with Red Sea coastal sites.* Renewable Energy, 1991. **1**(3-4): p. 435-440.
9. Fadare, D., *Modelling of solar energy potential in Nigeria using an artificial neural network model.* Applied energy, 2009. **86**(9): p. 1410-1422.
10. Mubiru, J., Banda, E. J. K. B., D'Ujanga, F., and T. Senyonga. *Assessing the performance of global solar radiation empirical formulations in Kampala, Uganda*. *Theor Appl Climatol*, 2007, **87**(1–4):179–184. https://doi.org/10.1007/s00704-005-0196-2.
11. Rijks, D. A., and P. A. Huxley, *The empirical relation between solar radiation and hours of bright sunshine near Kampala, Uganda. J Appl Ecol*, 1964. https://doi.org/10.2307/2401317.
12. Rahimikhoob, A., S. Behbahani, and M. Banihabib, *Comparative study of statistical and artificial neural network's methodologies for deriving global solar radiation from NOAA satellite images.* International journal of climatology, 2013. **33**(2): p. 480-486.
13. Angela, K., S. Taddeo, and M. James, *Predicting global solar radiation using an artificial neural network single-parameter model.* Advances in Artificial Neural Systems, 2011. **2011**.
14. Sözen, A., E. Arcaklıoğlu, M. Özalp, and N. Çağlar, *Forecasting based on neural network approach of solar potential in Turkey.* Renewable Energy, 2005. **30**(7): p. 1075-1090.
15. Yadav, A.K. and S. Chandel, *Solar energy potential assessment of western Himalayan Indian state of Himachal Pradesh using J48 algorithm of WEKA in ANN based prediction model.* Renewable Energy, 2015. **75**: p. 675-693.
16. Khatib, T., A. Mohamed, M. Mahmoud, and K. Sopian, *Modeling of daily solar energy on a horizontal surface for five main sites in Malaysia.* International Journal of Green Energy, 2011. **8**(8): p. 795-819.
17. Bilgili, M. and M. Ozgoren, *Daily total global solar radiation modeling from several meteorological data.* Meteorology Atmospheric Physics, 2011. **112**(3-4): p. 125.
18. Mbiaké, R., A.B. Wakata, E. Mfoumou, E. Ndjeuna, L. Fotso, E. Tiekwe, J.K. Djamen, and C. Bobda, *The Relationship between Global Solar Radiation and Sunshine Durations in Cameroon.* Open Journal of Air Pollution, 2018. **7**(2): p. 107-119.
19. Onyango, A.O. and V. Ongoma, *Estimation of mean monthly global solar radiation using sunshine hours for Nairobi City, Kenya.* Journal of renewable sustainable energy, 2015. **7**(5): p. 053105.

20. Cotfas, D.T., P.A. Cotfas, E. Kaplani, and C. Samoila, *Monthly average daily global and diffuse solar radiation based on sunshine duration and clearness index for Brasov, Romania.* Journal of Renewable Sustainable Energy, 2014. **6**(5): p. 053106.
21. Khatib, T., A. Mohamed, and K. Sopian, *A review of solar energy modeling techniques.* Renewable Sustainable Energy Reviews, 2012. **16**(5): p. 2864-2869.
22. Li, H., W. Ma, Y. Lian, X. Wang, and L. Zhao, *Global solar radiation estimation with sunshine duration in Tibet, China.* Renewable energy, 2011. **36**(11): p. 3141-3145.
23. Noguchi, Y., *Solar radiation and sunshine duration in East Asia.* Archives for meteorology, geophysics, bioclimatology, Series B, 1981. **29**(1-2): p. 111-128.
24. Ajayi, O., O. Ohijeagbon, C. Nwadialo, and O. Olasope, *New model to estimate daily global solar radiation over Nigeria.* Sustainable Energy Technologies Assessments, 2014. **5**: p. 28-36.
25. Karim, S.A.A., B.S.M. Singh, R. Razali, and N. Yahya. *Data compression technique for modeling of global solar radiation*. in *2011 IEEE International Conference on Control System, Computing and Engineering*. 2011. IEEE.
26. Bayrakçı, H.C., C. Demircan, and A. Keçebaş, *The development of empirical models for estimating global solar radiation on horizontal surface: A case study.* Renewable Sustainable Energy Reviews, 2018. **81**: p. 2771-2782.
27. Wang, L., O. Kisi, M. Zounemat-Kermani, Z. Zhu, W. Gong, Z. Niu, H. Liu, and Z. Liu, *Prediction of solar radiation in China using different adaptive neuro-fuzzy methods and M5 model tree.* International Journal of Climatology, 2017. **37**(3): p. 1141-1155.
28. Mohajeri, N., G. Upadhyay, A. Gudmundsson, D. Assouline, J. Kämpf, and J.-L. Scartezzini, *Effects of urban compactness on solar energy potential.* Renewable Energy, 2016. **93**: p. 469-482.
29. Lockart, N., D. Kavetski, and S.W. Franks, *A new stochastic model for simulating daily solar radiation from sunshine hours.* International Journal of Climatology, 2015. **35**(6): p. 1090-1106.
30. Benghanem, M. and A. Mellit, *A simplified calibrated model for estimating daily global solar radiation in Madinah, Saudi Arabia.* Theoretical applied climatology, 2014. **115**(1-2): p. 197-205.
31. Redweik, P., C. Catita, and M. Brito, *Solar energy potential on roofs and facades in an urban landscape.* Solar Energy, 2013. **97**: p. 332-341.
32. Adhikari, K.R., B.K. Bhattarai, and S. Gurung, *Estimation of global solar radiation for four selected sites in Nepal using sunshine hours, temperature and relative humidity.* Journal of Power Energy Engineering, 2013. **1**(03): p. 1.
33. Badescu, V., C.A. Gueymard, S. Cheval, C. Oprea, M. Baciu, A. Dumitrescu, F. Iacobescu, I. Milos, and C. Rada, *Accuracy analysis for fifty-four clear-sky solar radiation models using routine hourly global irradiance measurements in Romania.* Renewable Energy, 2013. **55**: p. 85-103.
34. Iizumi, T., M. Nishimori, M. Yokozawa, A. Kotera, and N. Duy Khang, *Statistical downscaling with Bayesian inference: Estimating global solar radiation from reanalysis and limited observed data.* International journal of climatology, 2012. **32**(3): p. 464-480.
35. Lee, K.H., *Constructing a non-linear relationship between the incoming solar radiation and bright sunshine duration.* International journal of climatology, 2010. **30**(12): p. 1884-1892.
36. Kumar, R. and L. Umanand, *Estimation of global radiation using clearness index model for sizing photovoltaic system.* Renewable energy, 2005. **30**(15): p. 2221-2233.
37. Couderc, E., *Solar energy: Hotspots in Tanzania.* Nature Energy, 2017. **2**(7): p. 1-1.
38. Ramachandra, T., R. Jain, and G. Krishnadas, *Hotspots of solar potential in India.* Renewable sustainable energy reviews, 2011. **15**(6): p. 3178-3186.
39. Šúri, M. and J. Hofierka, *A new GIS-based solar radiation model and its application to photovoltaic assessments.* Transactions in GIS, 2004. **8**(2): p. 175-190.
40. Aly, A., S.S. Jensen, and A.B. Pedersen, *Solar power potential of Tanzania: Identifying CSP and PV hot spots through a GIS multicriteria decision making analysis.* Renewable Energy, 2017. **113**: p. 159-175.

41. Salcedo-Sanz, S., C. Casanova-Mateo, J. Muñoz-Marí, and G. Camps-Valls, *Prediction of daily global solar irradiation using temporal Gaussian processes.* IEEE Geoscience Remote Sensing Letters, 2014. **11**(11): p. 1936-1940.
42. Zhang, Y., B. Qin, and W. Chen, *Analysis of 40 year records of solar radiation data in Shanghai, Nanjing and Hangzhou in Eastern China.* Theoretical Applied Climatology, 2004. **78**(4): p. 217-227.
43. Mundu, M.M., S.N. Nnamchi, and K.J. Ukagwu, *Algorithmized Modelling, Simulation and Validation of Clearness Index in Four Regions of Uganda.* Journal of Solar Energy Research, 2020. **5**(2): p. 432-452.
44. Nnamchi, S., O. Sanya, K. Zaina, and V. Gabriel, *Development of dynamic thermal input models for simulation of photovoltaic generators.* International Journal of Ambient Energy, 2018: p. 1-13.
45. Azdy, R.A. and F. Darnis. *Use of Haversine Formula in Finding Distance Between Temporary Shelter and Waste End Processing Sites*. in *Journal of Physics: Conference Series*. 2020.
46. Prasetya, D.A., P.T. Nguyen, R. Faizullin, I. Iswanto, and E.F. Armay, *Resolving the Shortest Path Problem using the Haversine formula.* Journal of Critical Reviews, 2020. **7**(1): p. 62-64.
47. Maria, E., E. Budiman, H. Haviluddin, and M. Taruk. *Measure distance locating nearest public facilities using Haversine and Euclidean Methods*. 2020. IOP-Journal of Physics: Conference Series.
48. Saputra, K., N. Nazaruddin, D.H. Yunardi, and R. Andriyani. *Implementation of haversine formula on location based mobile application in Syiah Kuala University*. in *2019 IEEE International Conference on Cybernetics and Computational Intelligence (CyberneticsCom)*. 2019. IEEE.
49. Monawar, T., S.B. Mahmud, and A. Hira. *Anti-theft vehicle tracking and regaining system with automatic police notifying using Haversine formula*. in *2017 4th International Conference on Advances in Electrical Engineering (ICAEE)*. 2017. IEEE.
50. Nestola, F. and J.R. Smyth, *Diamonds and water in the deep Earth: a new scenario.* International Geology Review, 2016. **58**(3): p. 263-276.
51. Matioc, A.-V., *Exact geophysical waves in stratified fluids.* Applicable Analysis, 2013. **92**(11): p. 2254-2261.
52. Trishchenko, A.P. and L. Garand, *Observing polar regions from space: advantages of a satellite system on a highly elliptical orbit versus a constellation of low Earth polar orbiters.* Canadian Journal of Remote Sensing, 2012. **38**(1): p. 12-24.